M. Giulbudagian | G. Yealland | S. Hönzke | A. Edlich |
B. Geisendörfer | B. Kleuser | S. Hedtrich | M. Calderón

Breaking the Barrier

Potent Anti-Inflammatory Activity following Efficient Topical Delivery of Etanercept using Thermoresponsive Nanogels

Suggested citation referring to the original publication:
Theranostics 8 (2018) 2, 450-463
DOI https://doi.org/10.7150/thno.21668
ISSN (online) 1838-7640

IVYSPRING INTERNATIONAL PUBLISHER

Theranostics

2018; 8(2): 450-463. doi: 10.7150/thno.21668

Research Paper

Breaking the Barrier – Potent Anti-Inflammatory Activity following Efficient Topical Delivery of Etanercept using Thermoresponsive Nanogels

M. Giulbudagian[1]*, G. Yealland[2]*, S. Hönzke[2], A. Edlich[3], B. Geisendörfer[3], B. Kleuser[3], S. Hedtrich[2]✉, M. Calderón[1]✉

1. Freie Universität Berlin, Institute of Chemistry and Biochemistry, Takustrasse 3, 14195 Berlin, Germany;
2. Freie Universität Berlin, Institute for Pharmacy (Pharmacology and Toxicology), Königin-Luise-Str. 2+4, 14195 Berlin, Germany;
3. University of Potsdam, Institute of Nutritional Science, Department of Nutritional Toxicology, Arthur-Scheunert-Allee 114-116, 14558 Nuthetal, Germany.

* These authors contributed equally to this work

✉ Corresponding authors: caldera@zedat.fu-berlin.de and sarah.hedtrich@fu-berlin.de

Received: 2017.06.28; Accepted: 2017.10.05; Published: 2018.01.01

Abstract

Topical administration permits targeted, sustained delivery of therapeutics to human skin. Delivery to the skin, however, is typically limited to lipophilic molecules with molecular weight of < 500 Da, capable of crossing the *stratum corneum*. Nevertheless, there are indications protein delivery may be possible in barrier deficient skin, a condition found in several inflammatory skin diseases such as psoriasis, using novel nanocarrier systems.

Methods: Water in water thermo-nanoprecipitation; dynamic light scattering; zeta potential measurement; nanoparticle tracking analysis; atomic force microscopy; cryogenic transmission electron microscopy; UV absorption; centrifugal separation membranes; bicinchoninic acid assay; circular dichroism; TNFα binding ELISA; inflammatory skin equivalent construction; human skin biopsies; immunohistochemistry; fluorescence microscopy; western blot; monocyte derived Langerhans cells; ELISA

Results: Here, we report the novel synthesis of thermoresponsive nanogels (tNG) and the stable encapsulation of the anti-TNFα fusion protein etanercept (ETR) (~150 kDa) without alteration to its structure, as well as temperature triggered release from the tNGs. Novel tNG synthesis without the use of organic solvents was conducted, permitting *in situ* encapsulation of protein during assembly, something that holds great promise for easy manufacture and storage. Topical application of ETR loaded tNGs to inflammatory skin equivalents or tape striped human skin resulted in efficient ETR delivery throughout the SC and into the viable epidermis that correlated with clear anti-inflammatory effects. Notably, effective ETR delivery depended on temperature triggered release following topical application.

Conclusion: Together these results indicate tNGs hold promise as a biocompatible and easy to manufacture vehicle for stable protein encapsulation and topical delivery into barrier-deficient skin.

Key words: thermoresponsive-nanogel, topical, anti-inflammatory therapy, etanercept, skin equivalents.

Introduction

Topical administration permits highly targeted, sustained delivery of therapeutics to the skin whilst circumventing many issues associated with systemic administration such as first pass metabolism and off target drug distribution. However, the outermost layer of human skin - the *stratum corneum* (SC) - is a highly effective barrier that prevents the penetration of all but small (< ~500 Da) and moderately lipophilic molecules.[1, 2] Nonetheless, several non-invasive techniques that facilitate the passage of hydrophilic macromolecules into or through skin have been tested. These include chemical penetration enhancers, [3-5] physical disruptions of the SC,[6-8] skin penetrating peptides [9-11] and a number of nanoparticles.[12-17] However, their ability to deliver large molecular weight (Mw) proteins, whilst

preserving the protein's biological activity and avoiding skin irritancy, remains an unattained goal.

Topical delivery of therapeutic macromolecules may present new therapeutic options for skin disorders. Common inflammatory skin diseases such as psoriasis and atopic dermatitis (AD) for instance may benefit from local, non-systemic applications of the ever-growing list of anti-inflammatory biologicals. This would circumvent the often severe side-effects associated with their systemic applications and would likely reduce the dose required of these highly expensive therapies.

Therapeutically useful topical protein delivery strategies must effectively deliver their cargo past the SC whilst preserving the protein's structure / biological activity, without damage to the existing skin barrier or induction of irritancy and cellular toxicity. These points limit the potential usefulness of some of the aforementioned skin delivery strategies for biomacromolecules. For example, though physical methods like sonoporation and microneedle patches can effectively deliver proteins into skin, the inherent energy involved can lead to conformational changes detrimental to the therapeutic activity of proteins as well as skin irritancy.[18]

Our groups have intensively investigated the potential of thermoresponsive nanogels (tNGs) as cutaneous penetration enhancers. They consist of nanometer scale polymeric networks incorporating thermoresponsive polymers that bestow environmental responsiveness to physiologically relevant changes in temperature.[19, 20] While they are swollen with water below their cloud point temperature (Tcp), the thermoresponsive polymers of the tNGs undergo a reversible transition in water solubility when exposed to greater temperatures, resulting in gel shrinking and the expulsion of water. A broad range of cargoes may be encapsulated within tNG and then released from these in a temperature sensitive manner.

The synthesis strategy of tNG has to take into consideration the compatibility with biologically active macromolecules, while retaining their structural integrity and biological activity. The nanoprecipitation technique is the method of choice for *in situ* protein encapsulation due to the absence of extensive shear forces, sonication or heating. Organic solvents such as dimethyl sulfoxide, acetonitrile, and acetone have been used as solvent components for protein encapsulation during nanoprecipitation [21-23]. Yet, the presence of such organic solvents might cause structural alterations to the protein and cause immunogenic responses owing to the presence of residual solvents. Here, we present a novel and universal technique for the fabrication of tNG under mild conditions that does not require the utilisation of organic solvents, surfactants, or elevated temperatures that would otherwise denature proteins. Here, the conventional method of nanoprecipitation, in which solvents and non-solvents are utilised for the particulate precipitation of polymeric precursors, was modified to allow an aqueous buffer solution to serve as both solvent and non-solvent. For this, dendritic polyglycerol (dPG) and linear thermoresponsive polyglycerol (tPG) served as building blocks for the fabrication of the tNGs. These, alongside the previously reported poly(N-isopropylacrylamide) (pNIPAM) based tNGs, were used to encapsulate etanercept (ETR). ETR is a fusion protein of the human TNFα receptor and the Fc tail of IgG1 (Mw ~150 kDa) approved for the treatment of psoriasis and arthritis by subcutaneous injection.[24, 25] Notably, the efficacy of human-based biologicals such as ETR cannot be easily tested in animals due to immunological responses. Hence, we utilized a previously established *in vitro* model of TNFα mediated skin inflammation - a key feature of inflammatory diseases such as psoriasis and chronic atopic dermatitis—and further characterise it for use as a novel preclinical test system.[26-28] With this and *ex vivo* human skin, we demonstrate the effective topical delivery of ETR to the viable epidermis (VE) by tNGs, followed by clear anti-inflammatory actions. We also demonstrate the necessity for triggered release of proteins from tNGs for their delivery into the VE following topical application. Furthermore, studies with immune cells akin to those found resident with human skin showed no toxic or immunogenic potential from the ETR loaded tNGs.[29]

Materials and Methods

Materials

Commercially available chemicals from standardised sources were used as delivered. Solvents were purchased as reagent grade and distilled if necessary. Anhydrous solvents were either purchased as ultra-dry solvent (Acros Organics®) or obtained from MBRAUN SPS 800 solvent purification system (Garching, Germany). Water was purified by a Millipore water purification system. Dendritic polyglycerol (dPG) with average Mw of 10 kDa (PDI = 1.27) was purchased from Nanopartica GmbH (Berlin, Germany). The crosslinking reagent (1R,8S,9s)-bicyclo[6.1.0]non-4-yn-9-ylmethyl (4-nitrophenyl) carbonate (BCN) was purchased from Synaffix (AE Oss, Netherlands).[30] Amine functionalization of dPG was performed according to a previously reported protocol [31]; degrees of functionalization

for dPG-$Ac_{10\%}$ and dPG-$BCN_{8\%}$ are given as a percentage of the total dPG hydroxyl groups (~ 135 hydroxyl groups for 10 kDa dPG). Glycidyl methyl ether (GME) (85%) and ethyl glycidyl ether (EGE) (98%; both TCI Europe, Eschborn, Germany) were dried over CaH_2, distilled, and stored over molecular sieves (5 Å). Indodicarbocyanine (IDCC) was purchased from Lumiprobe GmbH (Hannover, Germany). Synthesis of tPG was performed according to a previously reported procedure with slight adjustments.[32] Bovine Collagen I ("PureCol") was purchased from Advanced Biomatrix (San Diego, USA). Transwell cell culture inserts (3 µm pore molecular weight cut-off (MWCO)) were purchased from BD Biosciences (Heidelberg, Germany). Recombinant TNFα was purchased from Affymetrix eBiosciences GmbH (Frankfurt, Germany). For primary antibodies, anti-TNFα (ab183896), anti-TSLP (ab47943), and anti-ICAM1 (ab53013) were purchased from abcam (Cambridge, UK). For secondary antibodies, anti-IgG rabbit tagged with alexa 594 (ab10080) was purchased from abcam (Cambridge, UK), and anti-IgG rabbit tagged with horseradish-peroxidase (#7074) was purchased from Cell Signaling (Frankfurt/Main, Germany).

Synthesis and characterization of nanogels

The synthesis of pNIPAM-based nanogels (tNG_pNIPAM) was performed according to a previously reported method.[33] Briefly, pNIPAM (66 mg), acrylated dendritic polyglycerol (dPG-$Ac_{10\%}$) (33 mg), sodium dodecyl sulfate (SDS) (1.8 mg), and ammonium persulfate (APS) (2.8 mg) were dissolved in 5 mL of distilled water. To produce fluorescently labelled nanogels, indodicarbocyanine (IDCC) conjugated dPG-$Ac_{10\%}$ (3 mg) was allowed to react with the unlabeled crosslinker. Argon was bubbled into the reaction mixture for 15 min, followed by stirring under an argon atmosphere for another 15 min. The reaction mixture was then transferred into a water bath at 68 °C. Polymerization was activated after 5 min by addition of a catalytic quantity of N,N,N′,N′-tetramethylethane-1,2-diamine (TEMED; 120 µL). The mixture was stirred at 500 rpm for at least 4 h.

For the synthesis of tPG-based nanogels (tNG_tPG), dPG-$BCN_{8\%}$ (10 mg) and di-azide functionalised tPG (tPG-$(N_3)_2$) (20 mg) (and 0.3 mg ETR for *in situ* encapsulation) were mixed in 1 mL phosphate buffered saline (PBS), cooled in an ice bath and injected by syringe into 20 mL of PBS at 37 °C. The mixture was stirred for 6 h. Unreacted alkynes were quenched with azidopropanol or, alternatively, IDCC-N_3. The tNGs products were purified by dialysis (MWCO 50 kDa) in water for at least two days. In addition, IDCC labelled nanogels were purified by a Sephadex G25 fine column (GE Healthcare Berlin, Germany). The absence of a free dye was verified by thin layer chromatography (TLC) (Merck aluminium sheets with silica (corn size 60) and fluorescence marker F254).

The resulting tNG_pNIPAM was then lyophilised to yield a white solid. The tNG_tPG were stored as a highly concentrated solution. In total, three batches were produced and characterised independently.

Dynamic light scattering (DLS) and zeta potential

Size distribution and zeta potential of tNGs were measured at various temperatures by dynamic light scattering (DLS) using a Zetasizer Nano-ZS 90 (Malvern, UK) equipped with a He–Ne laser (λ = 633 nm) under scattering angle of 173°. For equilibration, samples with the concentration of 1 mg/mL were maintained at the desired temperature for 5 min prior to testing. Particle size distributions are given as the average of three measurements from intensity distribution curves. As DLS measurements of the nanogels were monomodal in distribution, with autocorrelation functions showing a single exponential decay, the hydrodynamic diameters are reported from the intensity distribution curves.

Nanoparticle tracking analysis (NTA)

Size, particle concentration, and approximate Mw of the tNGs were measured by NTA using a Nanosight NS500 (Malvern Instruments, Malvern, UK). The samples were prepared by diluting 1000 times the solution prepared for DLS measurements. Particle sizes, concentration, and Mw are given as the average of three measurements.

Atomic force microscopy (AFM)

AFM measurements were recorded on a MultiMode 8 AFM equipped with a Nanoscope V controller (Veeco Instruments, Santa Barbara, California). The data were analyzed using NanoScope Analysis 1.3 software and statistical analyses were performed on 10 µm x 10 µm images. The tNGs aqueous solutions (2.5 mg/mL) were air dried on a Mica sheet. Samples were measured with Nano World tips, Soft Tapping Mode (SNK-10), with resonance frequency of 56-75 kHz and force constant of 0.24 N/m.

Cryogenic transmission electron microscopy (cryo-TEM)

A droplet (5 µL) of the sample solution was placed on hydrophilized (plasma treatment using a BALTEC MED 020 device (Leica Microsystems, Wetzlar, Germany), perforated carbon filmed grids

(Quantifoil Micro Tools GmbH, Jena, Germany). The excess fluid was blotted off to create an ultra-thin layer (typical thickness of 200-300 nm) of the solution that spans the holes of the supporting film. Samples were then immediately vitrified by propelling the grids into liquid ethane at its freezing point (-184 °C). The vitrified sample grids were transferred under liquid nitrogen, by the use of a Gatan (Pleasanton,CA, USA) cryo-holder (Model 626), into a Tecnai F20 TEM (FEI company, Oregon, USA) equipped with a field emission gun (FEG) and operated under a 160 kV acceleration voltage. Microscopy was carried out at -175 °C sample temperature using the microscope's low dose protocol at calibrated primary magnifications of 5k and 29k. The defocus was set to 9.81 µm (29k). Images were recorded on a 4k-Eagle CCD camera (FEI Company, Oregon, USA) at 2k resolution (binning 2).

Cloud point temperature (Tcp) determination by UV-Visible measurement

The Tcp were measured on a Lambda 950 UV/Vis/NIR spectrometer, Perkin Elmer Life and Analytical Sciences (Connecticut, USA) equipped with a temperature-controlled, six-position sample holder. Solutions of tNG in PBS (pH 7.4) were heated at 0.2 °C/min while monitoring both the transmission at 500 nm (1 cm path length) and the solution temperature (from 18 to 55 °C), as determined by the internal temperature probe. The Tcp of each nanogel was defined as the temperature at the inflection point of the normalised transmission curves.

Encapsulation and release studies

For protein encapsulation of ETR or fluorescein isothiocyanate labelled bovine serum albumin (FITC-BSA), tNG_pNIPAM or tNG_tPG nanogels (10 mg/mL) were swollen in a protein solution (1 mg/mL) for 24 h at 4 °C. The *in-situ* encapsulation of ETR was performed as a proof of concept and used for its structural characterization. For experiments on skin models, proteins were encapsulated post synthesis by swelling tNGs in protein solutions. The solutions were purified using Vivaspin 300 kDa for FITC-BSA or Vivaspin 1000 kDa for ETR (according to the manufacturer's instructions; Sartorius AG, Göttingen, Germany). Protein concentrations in the resulting exudates were then determined by UV measurements for FITC-BSA and by Bradford assay for ETR. The Bradford assay was conducting according to standard procedure: 100 mg Coomassie Brilliant Blue G250 was dissolved in 50 mL of ethanol, to which 100 mL of concentrated phosphoric acid was added, and the final volume was adjusted to 200 mL with MilliQ water. Absorbance was recorded at 595 nm. Release studies were conducted by incubating the tNGs with the encapsulated protein at different temperatures, following which, the released protein fraction was separated by a centrifugal filtering device. For this, 1 mL tNGs (10 mg/mL) containing FITC-BSA were placed in a Vivaspin 1000 kDa centrifugal filtering device, and centrifuged at certain time intervals, according to the manufacturer's instructions. The filtrate solution was taken for analysis (absorbance recorded at 492 nm) while replacing it with a fresh buffer.

Structural integrity and activity of etanercept

Circular dichroism

Circular dichroism (CD) spectra were recorded by using a Jasco J-810 spectropolarimeter (Jasco, Gross-Umstadt, Germany) equipped with a temperature controller (Jasco PTC-348W1 peltier thermostat) using 0.2 mm path length Quartz Suprasil cuvettes (Hellma, Müllheim, Germany). After background correction, spectra were averaged over three scans (λ = 195–240 nm; 0.5 nm intervals; 2 mm bandwidth; 4 s response time, 100 nm/min scanning speed).

Etanercept–TNFα binding assay

Following release and purification from tNGs (Vivaspin 500 MWCO 1000 kD, Sartorius, Göttingen, Germany), ETR concentration was determined by bicinchoninic acid assay (BCA) (Pierce™ BCA Protein Assay Kit, Thermo Scientific, Waltham, MA, USA). All samples were then adjusted to 10 ng/mL, and their TNFα binding affinity determined by a commercially available sandwich ELISA that incorporates plate bound TNFα (Sanquin, Diagnostic Services, Amsterdam, Netherlands). Results are expressed as the samples TNFα binding as a percentage of fresh ETR TNFα binding.

Inflammatory skin equivalents and etanercept treatment

Skin equivalent construction and ETR application

Human skin equivalents were prepared from primary human keratinocytes and fibroblasts as previously described.[26, 34] Primary skin cells were derived from normal human skin with written consent. To induce skin inflammation, 20 ng/mL recombinant TNFα (eBioscience, Hatfield, UK) was supplemented into the skin equivalents growth media on days 10 and 12 of cultivation. ETR formulated in PBS (35 µg/cm²) or tNGs (35 µg/cm² ETR; 350 µg/cm² tNG) was applied topically on days 11 and 13 and exposed to a temperature ramp (32–37 °C) over 3 h. On day 14, skin equivalents were halved and

prepared separately for western blotting and immuno-histochemistry.

Western Blotting

Halved skin equivalents were lysed in RIPA buffer (supplemented with protease and phosphatase inhibitors) according to standard procedure. Protein content was quantified by BCA assay. Samples (15 µg protein) were then heated in SDS-PAGE buffer and separated by electrophoresis through a polyacrylamide gel (10%). Gels were blotted onto nitrocellulose membranes, blocked (5% skimmed-milk powder), exposed to primary antibodies (overnight, 4 °C), washed, incubated with horseradish peroxidise conjugated secondary antibodies (1 h, room temperature) and washed again. Blots were developed with ECL reagent (SignalFire™, Cell Signaling, Frankfurt/Main, Germany) and imaged by a PXi/PXi Touch gel imaging system (Syngene, Cambridge, UK). Antibodies were used at the following concentrations: 1:1000 anti-TNFα, 1:1000 anti-TSLP, anti-ICAM1 1:2000, 1:500 anti-IgG Rabbit conjugated to horseradish peroxidase.

Immunohistochemistry

Halved skin equivalents were submerged in tissue freezing media, and flash frozen. Samples were subsequently cut into cross sections (8 µm) on a cryotome (Leica, PLACE) against the direction of tNG application (i.e., deep to superficial). Skin sections were fixed using a 4% formaldehyde solution, washed with PBS containing 0.0025% BSA and 0.025% Tween 20 and blocked with goat serum (1:20 in PBS). Subsequently, skin sections were incubated overnight at 4 °C with primary antibodies. After washing, secondary antibodies were added for 1 h at room temperature, and finally skin sections were covered with antifading mounting medium. Images were analysed under a fluorescence microscope (BZ-8000, objectives 20x/0.75, zoom 10x, Plan-Apo, DIC N2, Keyence, Neu-Isenburg, Germany). Antibodies were used at the following concentrations: 1:500 anti-TNFα, 1:500 anti-IgG Rabbit conjugated to Alexa 594.

Immunological response of Langerhans cells after incubation with tNGs

Monocyte derived Langerhans cells (MoLC) were generated from isolated human monocytes as described elsewhere.[35] Following seven days cultivation, MoLC were collected and characterized by surface expression of CD1a and CD207.[35] Afterwards, MoLCs were seeded into 24-well plates (2.5×10^5 cells/well) and incubated with tNGs (0.1 and 0.5 mg/mL, with or without ETR load) for 24 h. The immunogenic effects of the tNGs were determined by the cell-surface expression CD83 and CD86 as described previously.[35] Additionally, cytotoxicity was measured by staining the cells with 7-Aminoactinomycin D (7-AAD) (Sigma-Aldrich, Munich, Germany). Surface receptor expression and 7-AAD penetration was assessed by flow cytometry (FACSCanto II, BD Biosciences, Heidelberg, Germany) and the resulting data analysed by FlowJo software (Treestar, Ashland, USA).

Results and Discussion

Synthesis and characterization of thermoresponsive nanogels formed by water in water thermo-nanoprecipitation

The structural integrity of therapeutic proteins must be preserved when encapsulated within synthetic delivery vectors, as well as during their subsequent release, to ensure their biological activity. Moreover, the presence of certain substances originating from the initial synthesis procedure could strongly impact upon subsequent therapeutic action as a consequence of modification to protein structure or direct cellular toxicity. The encapsulation of proteins in crosslinked polymeric network is often performed *in situ* (i.e., during particle formation) to ensure efficient encapsulation. This requires very mild reaction conditions and above all bio-orthogonality towards the bioactive compound; elevated temperatures, the utilization of organic solvents and surfactants should all be avoided. Therefore, we were motivated to establish a modular approach to allow the *in situ* encapsulation of proteins in a framework of thermoresponsive nanogels.

One of the most suitable methodologies for nanoparticle assembly from macromolecular precursor monomers is the nanoprecipitation technique.[21, 36, 37] This method is based on the injection of concentrated polymer solution into a non-solvent for the polymer that is also miscible with the polymer solvent. Our group has recently established a system where water held above the transition temperature of the corresponding thermoresponsive polymer could be used as a non-solvent.[38] Here we present an advanced approach: water in water thermo-nanoprecipitation (Figure 1). Given the temperature dependent solubility of thermoresponsive polymers, water could be used as both the polymer solvent and non-solvent. The macromolecular precursor molecules dPG-$(BCN)_{8\%}$ and tPG-$(N_3)_2$ were solubilised in PBS, cooled in an ice bath, and then injected into PBS at 37 °C. The Tcp of the tPG used here was tuned to occur at 32 °C and as such, be fully soluble at 4°C. Exposure to temperatures > Tcp lead to polymer precipitation and the formation of precursor particles. Subsequently,

upon the bioorthogonal crosslinking reaction between the strained alkyne and the azide functionalized precursor polymers, tNGs could be formed.

Since the nanoprecipitation method is driven by the diffusion of the solvent into the non-solvent, the affinity of both dictates the diffusion rate and therefore the stability of the precursor suspension. The affinity of solvents towards each other (χ) can be described by the Hildebrand solubility parameter (δ), which in turn depends on temperature.[39] We believe that this dependency on temperature allows water at different temperatures to act as solvent and non-solvent for thermoresponsive polymers. Alternatively, the solvated polymer may precipitate upon the rapid heat transfer between the warm and the cold buffer solutions.

One parameter affecting the formation of stable colloidal suspensions is the method by which both solvents are exposed to each other.[36] Several protocols were screened, including injection, dropwise addition of the non-solvent to the solvent, and slow heating of polymeric precursor solutions. Of these, the most reproducible formation of tNGs was achieved by injection of 1 mL polymer-PBS solution (30 mg/mL) held at 4 °C into 20 mL PBS held at 37 °C. The formation of the precursor particles is also known to be strongly dependent on the concentration of polymer in solvent.[40] Concentrations of 1–30 mg/mL resulted in tNGs of comparable sizes and size distributions as confirmed by DLS, AFM and cryo-TEM analyses (Figure 2 a, b, c). This key parameter along with physiological reaction conditions allowed the co-precipitation of ETR, while retaining an unchanged tNG_tPG hydrodynamic diameter. Furthermore, NTA, which permits the determination of particle number, confirmed that increased polymer concentrations lead to proportional increases in the particle concentration, suggesting similar densities of tNG_tPG.

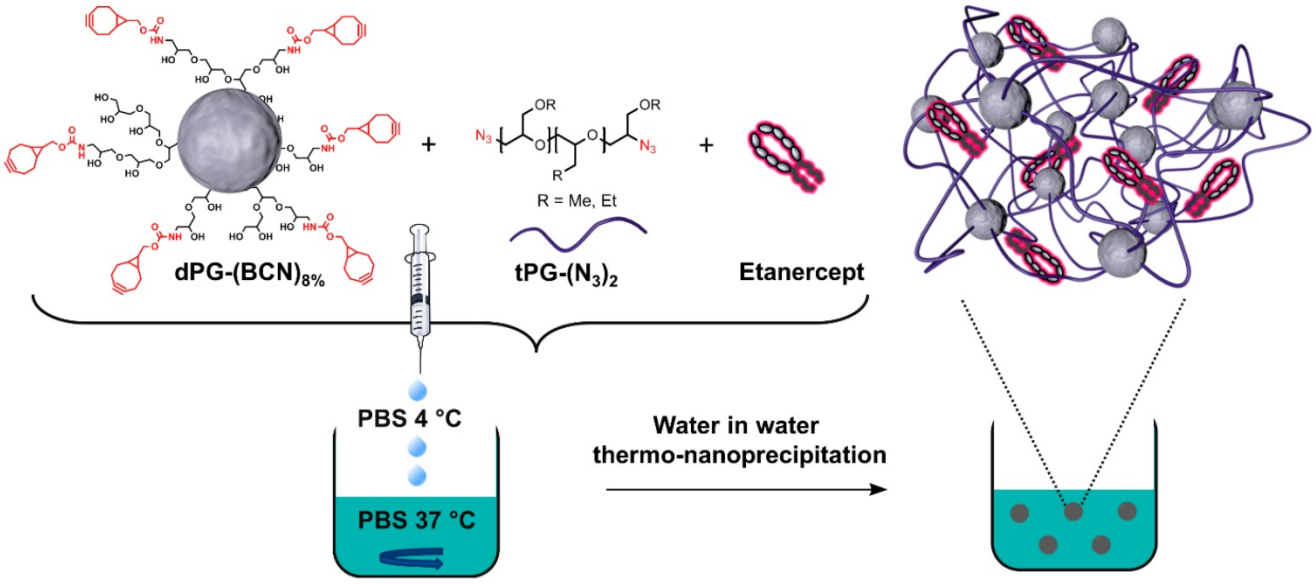

Figure 1. Schematic representation of the water in water thermo-nanoprecipitation technique and the precursor macromolecules. ETR is co-precipitated during particle formation.

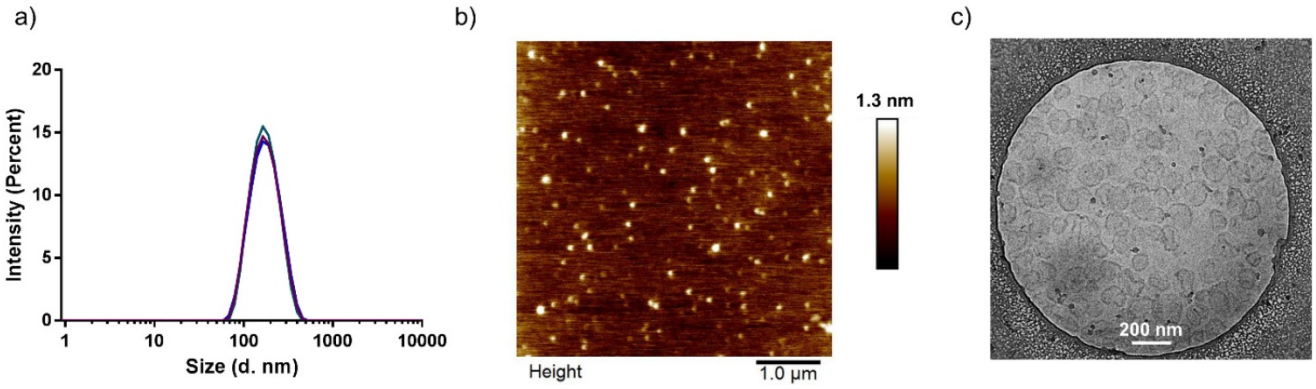

Figure 2. Characterization of tNG_tPG. a) DLS, presented as size distributions by intensity, b) AFM height profile (scale bar 1 µm), 155.16 ± 22.14 nm, and c) cryo-TEM image (scale bar 200 nm).

The skin penetration enhancing effects of two types of tNGs were assessed in the present study: tPG based tNGs synthesised as described above and pNIPAM based tNGs. Both use dPG as a macro-crosslinker to enable the growth of linear thermoresponsive polymers from a single core. The pNIPAM tNGs were synthesised by the well-established precipitation polymerization method from the acrylated dPG (dPG-Ac $_{10\%}$) and NIPAM to achieve tNG of the desired size (Table S1).

Encapsulation and release of etanercept by thermoresponsive nanogels

Encapsulation of ETR or the model protein FITC-BSA was achieved by swelling the tNGs in a solution of the corresponding protein. For the tNGs_pNIPAM, this involved addition of the protein solution to the lyophilised NGs. As the tNG_tPG were handled and stored in concentrated solution, encapsulation was achieved by addition of concentrated protein solution above tNG Tcp and subsequent incubation together below the Tcp. The encapsulation of ETR in both types of tNGs had no obvious effect on the Tcp of the corresponding carrier (Figure 3 a). Moreover, encapsulation shielded the negative Zeta potential of ETR (approximately -17 mV, 0.25 mg/mL) allowing the tNGs to retain their near neutral surface charges (Figure 3 b) [41]. Interestingly, the hydrodynamic diameter of both carriers remained unchanged upon encapsulation of ETR 10 wt. %. Together these data suggest efficient encapsulation of ETR within the crosslinked polymeric network of the tNGs.

To estimate *in vitro* release kinetics, FITC-BSA was encapsulated in both types of tNG and incubated at different temperatures. Released FITC-BSA was then separated from the tNGs suspension and quantified by UV-Vis (Figure 4). In their swollen state (25 °C), the tNGs showed good protein retention with a release plateau of 14.7 ± 3.2 % and 22.3 ± 4.3 % for tNG_pNIPAM and tNG_tPG respectively after 8 h (19.7 ± 4.0 % and 34.9 ± 4.6 % respectively after 48 h). When exposed to temperatures above their Tcp, the rate of protein release from the tNG_tPG was instead sustained following 3 h incubation, reaching 89.9 ± 8.9 % after 48 h. Above the Tcp of the tNG_pNIPAM, an immediate burst in protein release was seen, achieving 23.6 ± 5.6 % after just 1 h compared to 9.5 ± 5.3% below the Tcp. A plateau was then seen between 3 and 8 h, following which a linear phase of protein release was seen, achieving 82.4 ± 5.6 % after 48 h.

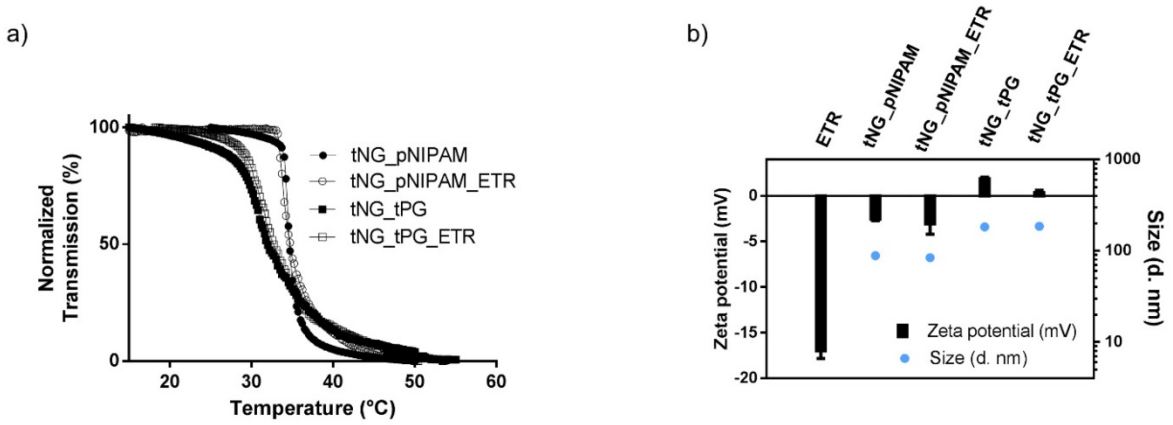

Figure 3. a) Normalised transmission of the tNGs aqueous solutions as a function of temperature UV-Vis (λ = 500 nm). b) Zeta potential and size of ETR and tNGs.

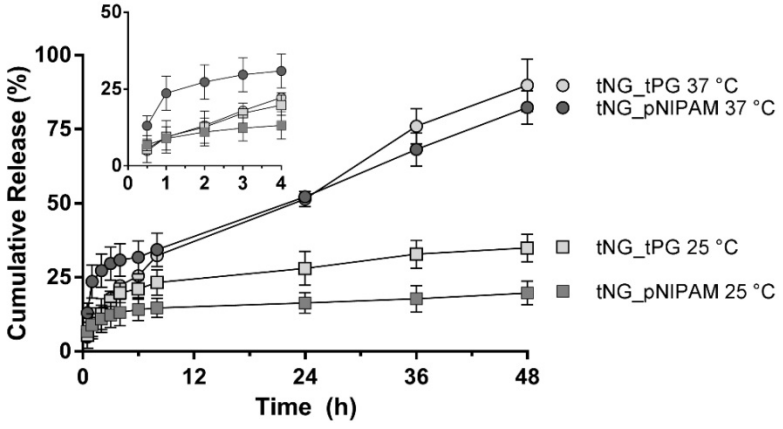

Figure 4. Cumulative release of FITC-BSA from tNG_pNIPAM and tNG_tPG at 25 °C and 37 °C. Inset shows release profiles over the first 4 h.

To ensure the structural stability of ETR within the tNGs, CD measurements were performed (Figure 5). Thermal denaturation of the protein was observed to occur at temperatures ≥ 45 °C, in line with previous literature [41, 42]. Therefore the mild reaction conditions in which the tNG_tNGs are synthesised (temperatures do not exceed 37 °C) will enable ETR encapsulation during tNG_tPG formation without loss of structural integrity, as well as by temperature induced swelling of pre-formed tNGs. Indeed, the CD spectra of encapsulated ETR in both types of tNGs showed no deviation from the native secondary structure.

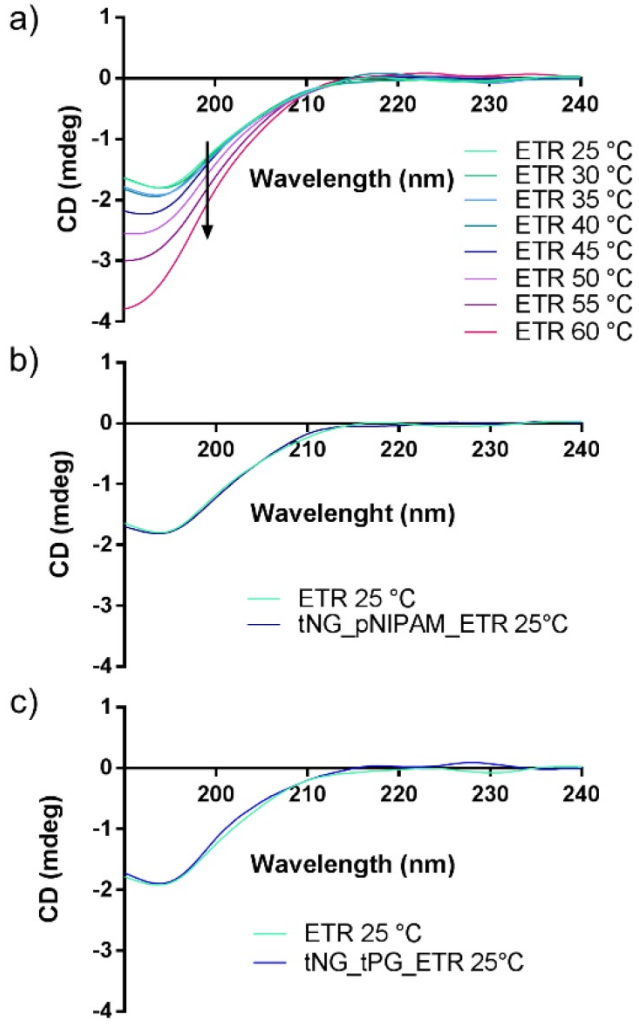

Figure 5. CD spectra of a) ETR measured at different temperatures. b) ETR encapsulated in tNG_pNIPAM, c) ETR encapsulated in tNG_tPG.

Previous literature has demonstrated encapsulation of proteins within tNGs better preserves their biological activity following release after long term storage.[12] Similar results for ETR have also been described following encapsulation in synthetic carriers.[43] An ELISA based assay of TNFα binding by ETR was performed following 0, 2 and 4 weeks storage at room temperature for ETR held in solution or encapsulated within tPG or pNIPAM based tNGs (Figure 6). While a significant decrease in TNFα binding was seen by the fourth week for ETR in PBS, the binding activity of ETR encapsulated in both tNG chemistries appeared stable throughout the tested duration. This is perhaps the result of weak interactions between ETR molecules and the encapsulating chemistries when concentrated within the tNG, acting to stabilise protein structure and shield them from environmental factors. Similarly, larger ETR concentrations have previously proven more stable.[41]

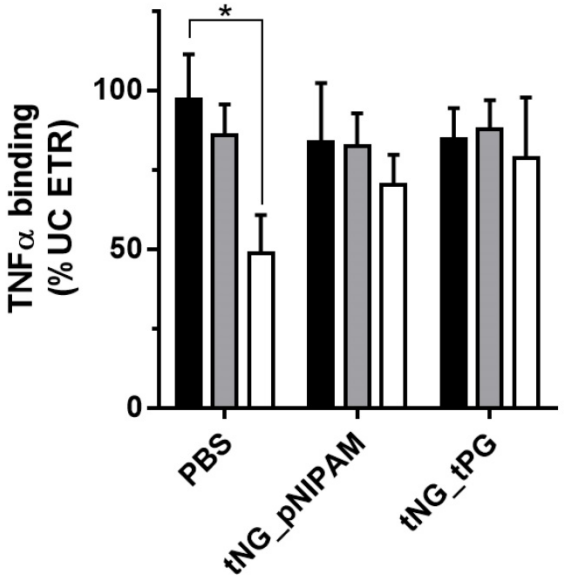

Figure 6. ETR–TNFα binding assay following 0 (black), 2 (grey) and 4 (white) weeks storage at room temperature. Statistical differences were calculated by multiple Student's *t* -test (error bars = SEM; * = $p \leq 0.05$).

Thermoresponsive nanogel mediated etanercept delivery to inflammatory skin equivalents

To assess the ability of the tNGs to deliver ETR past the SC and any local anti-inflammatory effects that result from this, penetration studies were performed in living human-based skin equivalents. In recent years, the importance of human-based model systems for basic and preclinical research has been increasingly recognised. In biomedical research of the skin and inflammatory diseases, results obtained from animal models have often held poor predictive value for humans owing to gross anatomical and physiological differences.[44, 45] Ultimately, this has resulted in a high rate of failure in the translation from preclinical to clinical studies.[46] For the testing of human-based biologicals such as ETR, animal studies appear even less adequate given the immediate

immune responses experienced upon administration of macromolecules derived from other species. Moreover, major concerns over the suitability of established models for assessing drug related effects were recently raised, in particular, the widely used imiquimod-induced murine psoriasis model. To induce an inflammation-like state, normal skin equivalents were supplemented with TNFα, a key mediator of plaque psoriasis and chronic atopic dermatitis.[28] As previously reported, this recapitulates several key features of inflammatory skin disease including hyperkeratosis, increased release of pro-inflammatory cytokines and unphysiologically high skin surface pH.[26, 27] However the reader should note the addition of TNFα alone to skin equivalents devoid of immune cells cannot fully emulate the complexity of the *in vivo* conditions.[47]

ETR in PBS alone or in tNGs was applied directly to the surface of skin equivalents 24 h after TNFα treatment (days 11 and 13) and exposed to a temperature gradient to simulate the natural temperature gradient of human skin (32–37 °C over 3 h) (Figure 7). On day 14, models were processed for immunohistochemical and western blot analyses. Application of tNG resulted in high ETR concentrations throughout the SC and apparent penetration into the VE (Figure 8). The effect was more pronounced in tNG_pNIPAM treated equivalents. In this regard, it is interesting to note the release kinetics from protein loaded tNG_pNIPAM at 37 °C markedly exceeded those of protein loaded tNG_tPG over the first hour of incubation (Figure 4). When applied in PBS, ETR failed to penetrate into the VE (Figure 8a). Though no quantitative measurements were made here, the effective delivery of ETR into the TNFα treated equivalents by the tNGs but not PBS shows the requirements for a potent delivery system.[48] Notably, the ability of tNG encapsulated ETR to overcome the SC suggests the presence of a moderate barrier deficiency similar to that observed in psoriasis and atopic dermatitis—in which enhanced skin permeabilities are characteristic—as well as other disease modelling skin equivalents.[12, 26, 49-51] Previous work from our group has demonstrated the effective tNG_pNIPAM mediated delivery of BSA (~68 kDa), Asparaginase ~140 kDa) and Transglutaminase 1 (~89 kDa) into the VE of tape stripped porcine skin, *filaggrin* knockdown skin equivalents, and *transglutaminase 1* knock-down skin equivalents respectively, all models of barrier-deficient skin.[12, 52] Notably, protein delivery to the viable layers of barrier intact skin was not possible. ETR (~150 kDa) is the largest protein yet to be effectively delivered to the VE of skin equivalents by tNG_pNIPAM and the first demonstration that protein loaded tNGs_tPG can achieve similar results. It is, however, notable that the permeability of skin equivalents to certain compounds is inherently greater than found *in vivo*. To address whether protein delivery is also possible in barrier deficient human skin, FITC-BSA loaded tPG and pNIPAM tNGs were applied onto tape stripped, excised human skin (Figure S1). Concordant with the data from the skin equivalents, protein penetration through the SC and into the VE were apparent.

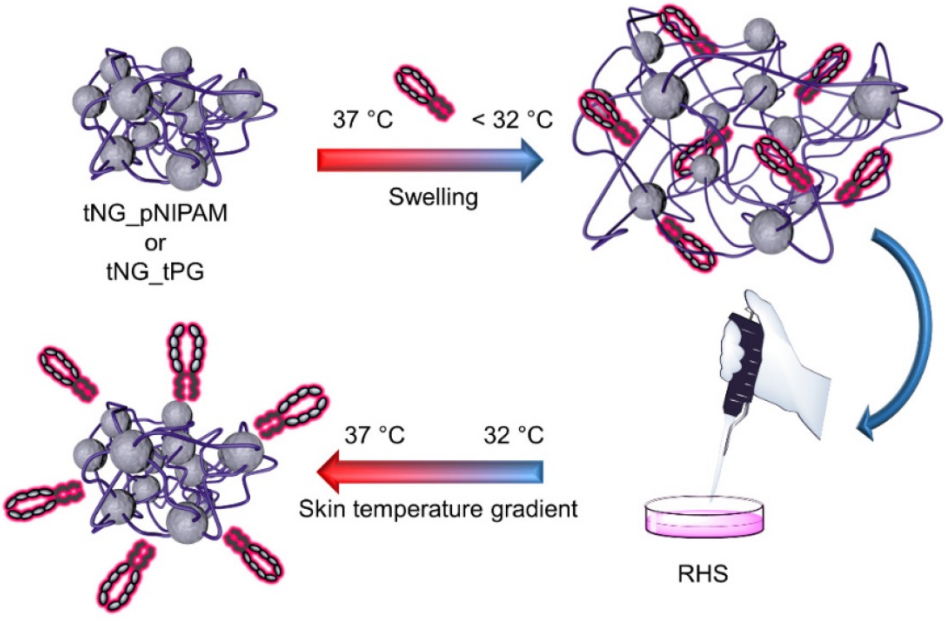

Figure 7. Experimental setup: ETR is encapsulated in tNG_pNIPAM or tNG_tPG by letting them swell in a solution of ETR, below the clouding point. Following, the tNGs are applied on reconstructed human skin (RHS) equivalents treated with TNFα (day 11 and 13) and incubated in a temperature gradient of 32-37 °C over 3 h, simulating the natural temperature gradient of human skin.

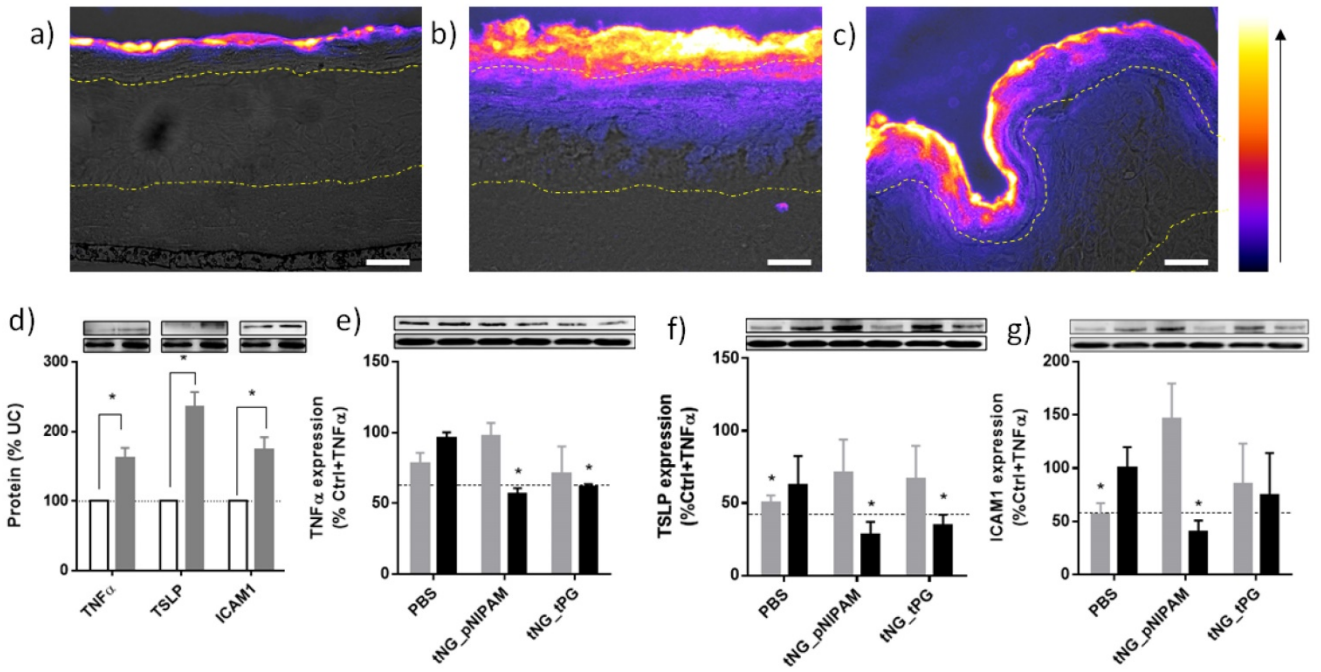

Figure 8. Representative immunohistochemical staining against ETR in skin equivalents topically treated with ETR dissolved in PBS (a) or encapsulated in tNG_pNIPAM (b) or tNG_tPG (c). Images show pseudo coloured ETR temperature staining (scale and direction of increasing signal intensity shown on the right) overlaid onto differential interference contrast (DIC) images, onto which the boundaries between the *stratum corneum* / viable epidermis (upper) and the viable epidermis / dermis (lower) have been marked (scale bar = 50 µm). Protein levels of TNFα, TSLP and ICAM1 in TNFα treated skin equivalents (black) calculated as a percentage of normal skin equivalents (grey) (d). Protein levels of TNFα (e), TSLP (f) and ICAM1 (g) in TNFα treated skin equivalents following treatment with empty (grey) or ETR loaded (black) tNGs or PBS. Values are expressed as a percentage of TNFα treated controls. Insets show representative western blots from the protein of interest, above, and β actin, below. Dashed lines indicate mean protein levels found in untreated, normal skin equivalents. Statistical differences from the normal controls (d) or TNFα treated controls (e-f) were calculated by Student's *t* -test (n = 3, error bars = SEM, * = $p \leq 0.05$).

The precise mechanism by which the tNGs are able to deliver proteins past the SC is not entirely clear. When FITC-BSA loaded in tNG based on p(N-isopropylmethacrylamide) (pNIPMAM) (Tcp = 47 °C) were applied to tape stripped skin, little to no penetration past the SC was observed (Figure S1a).[53] This indicates the temperature triggered release of protein, water, and/or heat induced conformational changes to the tNG structure are essential to the observed protein penetration into the skin. Indeed, we saw evidence that protein entered the VE of TNFα treated equivalents alone, while the tNGs remained exclusively in their SCs (Figure S2), concordant with other published data.

In a previous study, ultrastructural analyses of the SCs of skin biopsies following 2 h tNG_tPG exposure revealed clear disordering and/or swelling within the comprising structural components, as well as apparent dilations of the spaces between these.[54] This was strongly suggestive of an enhanced state of hydration within the SC.[55] It was also demonstrated that lipid to protein ratios found within the SC were increased following application of tNG_tPG and, to a lesser extent, tNG_pNIPAM. Thus, the penetration enhancing effects of the tNG correlated well with their ability to re-organise the SC, possibly forming transient pathways along which molecules may diffuse, a hypothesis that could rightly be applied to the present study. While we have demonstrated the necessity of skin barrier impairment and triggered protein/water release from the tNGs for effective protein delivery (Figure S1), the significance of protein release profiles from tNGs on the skin surface and/or in the SC will require more thorough quantitative investigations. It is however notable that the tNG tested here and elsewhere appear to show an innate ability to penetrate into the SC, or to interfere with its structural ordering, and that release from within the SC could significantly improve the penetration of proteins.[54] Future exploration of factors such as cross-linking density, rigidity, charge and hydrophilicity may prove insightful with regard to the SC penetrating properties of tNGs.[54, 56, 57]

In TNFα derived skin inflammation, keratinocytes of the VE are known to release several cytokines including thymic stromal lymphopoietin (TSLP) [49] and further TNFα. [58, 59] They also up-regulate cell surface receptors such as intercellular adhesion molecule 1 (ICAM1), a leukocyte adhesion molecule that plays a key role in plaque psoriasis.[60] Western blot analysis confirmed TNFα application induced similar responses in our skin equivalents (Figure 8d). Topical application of ETR in tNG_pNIPAM produced significant reductions in all

three proteins relative to TNFα treated skin equivalents, achieving levels found in the untreated skin equivalents (Figure 8e-g). Similar reductions in TNFα and TSLP levels were achieved following application of ETR in tNG_tPG. Interpretation of these results is, however, complicated by the apparent effects of the vehicle controls. For instance, application of PBS alone produced significant decreases in TSLP and ICAM1 levels, perhaps a result of water permeation into the equivalents and subsequent dilution of the extracellular environment in the VE.[1] Indeed, previous evidence has shown skin dehydration is associated with the upregulation of pro-inflammatory markers.[61] Though non-significant, deviations are also apparent for equivalents treated with empty tNGs. This may again relate to altered water contents within the skin equivalents, structural changes induced by tNGs, or occlusive effects induced by tNG presence on the equivalent's surface.[54] Nevertheless, the impact of ETR is clear, wherein its delivery by the tNGs correlated with the strongest and most consistent anti-inflammatory effects on the skin equivalents as is particularly notable in TSLP levels. Moreover, delivery of ETR in PBS results in less pronounced effects than applications of PBS alone, perhaps owing to the higher osmotic potential of the equivalents surface when proteins are applied. This highlights the particular effect tNG mediated ETR delivery has and suggests a mechanism that involves more than simple skin hydration.

Though we saw no robust evidence of tNG penetration past the SC in our skin equivalents at our tested time-points and concentrations, there is some evidence that this may be possible in *ex vivo* human skin, and that very small amounts of tNGs are actively taken up by dendritic cells of the VE, something that could prove valuable to the treatment of inflammatory skin diseases.[62, 63]

Immunogenicity

The human skin is a highly immunologically active organ. Many immune cells, such as Langerhans cells (LCs), reside and function as sentinels for potential harmful xenobiotics. Notably, proteins are also highly immunogenic and topical application of proteins requires a careful assessment of potential immunological activations that would limit their applicability. Additionally, interactions between tNGs and immune cells of the skin cannot be excluded. To date, it has been shown that both tNG_pNIPAM and tNG_tPG induce no specific toxicity in murine LC's or human keratinocytes.[63, 64] However, a lack of cytotoxicity does not exclude immunogenicity. Though nanoparticle induced immunogenicity is desirable in certain instances -vaccine formulations for example[65, 66] - further immune cell activation in inflammatory skin diseases is not.[67] Indeed, the bio- and immune- compatibility of the tNGs towards skin LCs is essential to their use in the topical treatment of a wide range of skin diseases.

Monocyte derived LCs (MoLC) were used to determine the bio- and immune- compatibility of the empty and ETR-loaded tNGs. Upon immunological activation, immature MoLC elevate surface expression of CD86 and CD83. Expressions of these markers were measured by flow cytometric analysis as an assay of immunogenicity. Following incubation with loaded and unloaded tNG_pNIPAM and tNG_tPG, as well as ETR in solution, the expressions of CD86 and CD83 were not significantly altered (Figure 9a, b). In addition, 7-AAD, a cell membrane impermeable dye, was used to assess MoLC viability, and demonstrated no cytotoxic induction (Figure 9c).

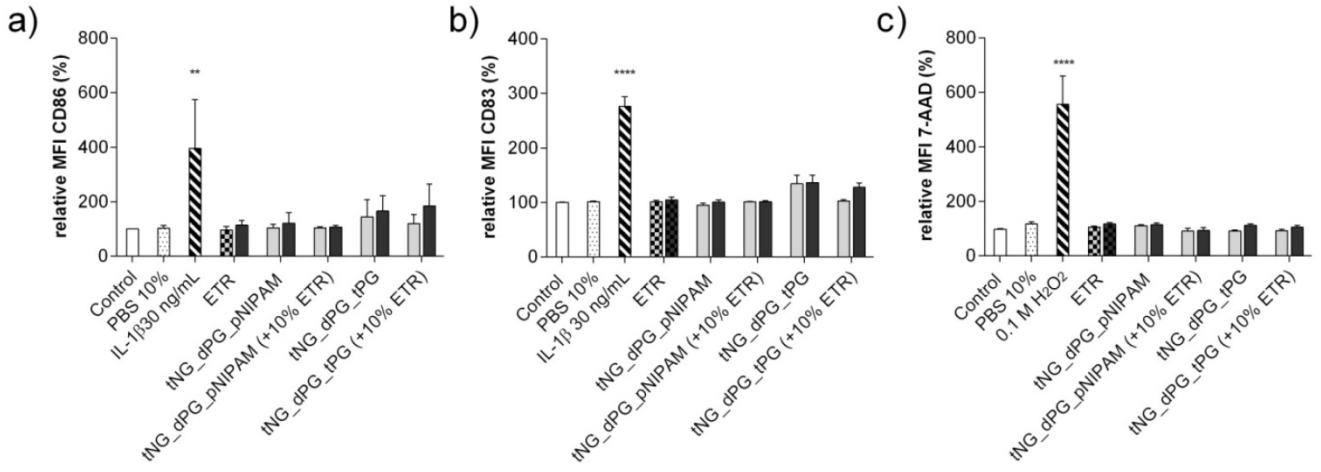

Figure 9. Expression of the activation markers (a) CD86 and (b) CD83 of MoLCs after 24 h incubation with unloaded and ETR-loaded tNGs and ETR in PBS (grey = 0.05 mg/mL ETR, black = 0.5 mg/mL ETR). (c) Cytotoxic induction in MoDCs, as measured by 7-AAD exclusion. Statistical differences from untreated control were calculated by one way ANOVA with Dunnett's correction for multiple comparisons (n = 3, error bars = SEM, ** = $p \leq 0.01$).

Conclusions

This proof–of-concept study holds major implications for tNG production as well as high throughput protein encapsulation strategies. Potentially, the herein presented methodology could be adapted for the fabrication of tNGs from a library of various thermoresponsive polymers. To the best of our knowledge, it is also the first strategy to show local anti-inflammatory activity within skin following topical protein application. Compared to systemic routes, topical administration of proteinaceous biologicals could prove advantageous in several regards: improved therapeutic targeting against dermatological conditions, reductions in off target effects and reductions in the therapeutic doses required of these costly therapies.

Abbreviations

AD: atopic dermatitis
AFM: atomic force microscopy
APS: ammonium persulfate
BSA: bovine serum albumin
cryo-TEM: cryogenic transmission electron microscopy
DIC: differential interference contrast
DLS: dynamic light scattering
dPG: dendritic polyglycerol
EGE: ethyl glycidyl ether
ETR: etanercept
FITC: fluorescein isothiocyanate
GME: glycidyl methyl ether
ICAM1: intercellular adhesion molecule 1
IDCC: indodicarbocyanine
IgG: Immunoglobulin G
kDa: kilo Dalton
LC: Langerhans cell
MoLC: monocyte derived Langerhans cell
Mw: molecular weight
MWCO: molecular weight cut-off
NTA: nanoparticle tracking analysis
PBS: phosphate buffered saline
PDI: polydispersity index
pNIPAM: poly(N-isopropylacrylamide)
pNIPMAM: p(N-isopropylmethacrylamide)
RHS: reconstructed human skin
SC: *stratum corneum*
SDS: sodium dodecyl sulfate
SEM: standard error of the mean
Tcp: cloud point temperature
TEMED: N,N,N′,N′-tetramethylethane-1,2-diamine
TLC: thin layer chromatography
TNFα: tumor necrosis factor alpha
tNG: thermoresponsive nanogel
tNG_pNIPAM: dendritic-polyglycerol-poly(N-isopropylacrylamide) thermoresponsive nanogels
tNG_tPG: dendritic-polyglycerol–thermoresponsive-polyglycerol thermoresponsive nanogels
tPG: thermoresponsive polyglycerol
TSLP: thymic stromal lymphopoietin
VE: viable epidermis

Acknowledgments

We gratefully acknowledge financial support from the Sonderforschungsbereich 1112, projects A04 (M.G., M.C.), C02 (S.Hö., S.He) and Z01 (A.E., B.G., B.K.), the Deutsche Forschungsgemeinschaft (DFG), HE 7440/4-1, the Berlin-Brandenburg Forschungsplattform BB3R and the Bundesministerium für Bildung und Forschung (BMBF) through the NanoMatFutur award (13N12561, Thermonanogele).

Supplementary Material

Supplemental table 1; details the sizes distributions, surface charges, cloud point temperatures and protein loads of the thermoresponsive nanogels.
Supplemental figure 1; shows the penetration of FITC-BSA into tape stripped *ex-vivo* human skin when applied topically in PBS or as a cargo of thermoresponsive nanogels. Supplemental figure 2; penetration of FITC–BSA encapsulated within rhodamine B labeled tNGs into skin equivalents following 3 h incubation.
http://www.thno.org/v08p0450s1.pdf

Competing Interests

The authors have declared that no competing interest exists.

References

1. Choy YB, Prausnitz MR. The Rule of Five for Non-Oral Routes of Drug Delivery: Ophthalmic, Inhalation and Transdermal. Pharm Res. 2011; 28: 943-8.
2. Bouwstra JA, Ponec M. The skin barrier in healthy and diseased state. Biochim Biophys Acta. 2006; 1758: 2080-95.
3. Magnusson BM, Runn P. Effect of penetration enhancers on the permeation of the thyrotropin releasing hormone analogue pGlu-3-methyl-His-Pro amide through human epidermis. Int J Pharm. 1999; 178: 149-59.
4. Karande P, Jain A, Mitragotri S. Discovery of transdermal penetration enhancers by high-throughput screening. Nat Biotech. 2004; 22: 192-7.
5. Karande P, Jain A, Mitragotri S. Insights into synergistic interactions in binary mixtures of chemical permeation enhancers for transdermal drug delivery. J Controlled Release. 2006; 115: 85-93.
6. Chen W, Li H, Shi D, Liu Z, Yuan W. Microneedles As a Delivery System for Gene Therapy. Front Pharmacol. 2016; 7: 137.
7. Prausnitz MR, Mitragotri S, Langer R. Current status and future potential of transdermal drug delivery. Nat Rev Drug Discov. 2004; 3: 115-24.
8. Kim Y-C, Ludovice PJ, Prausnitz MR. Transdermal delivery enhanced by magainin pore-forming peptide. J Controlled Release. 2007; 122: 375-83.
9. Hsu T, Mitragotri S. Delivery of siRNA and other macromolecules into skin and cells using a peptide enhancer. Proceedings of the National Academy of Sciences. 2011; 108: 15816-21.
10. Chen Y, Shen Y, Guo X, Zhang C, Yang W, Ma M, et al. Transdermal protein delivery by a coadministered peptide identified via phage display. Nat Biotechnol. 2006; 24: 455-60.
11. Vij M, Natarajan P, Pattnaik BR, Alam S, Gupta N, Santhiya D, et al. Non-invasive topical delivery of plasmid DNA to the skin using a peptide carrier. J Controlled Release. 2016; 222: 159-68.
12. Witting M, Molina M, Obst K, Plank R, Eckl KM, Hennies HC, et al. Thermosensitive dendritic polyglycerol-based nanogels for cutaneous

delivery of biomacromolecules. Nanomedicine: Nanotechnology, Biology and Medicine. 2015; 11: 1179-87.
13. Aufenvenne K, Larcher F, Hausser I, Duarte B, Oji V, Nikolenko H, et al. Topical Enzyme-Replacement Therapy Restores Transglutaminase 1 Activity and Corrects Architecture of Transglutaminase-1-Deficient Skin Grafts. American Journal of Human Genetics. 2013; 93: 620-30.
14. Desmet E, Bracke S, Forier K, Taevernier L, Stuart MC, De Spiegeleer B, et al. An elastic liposomal formulation for RNAi-based topical treatment of skin disorders: Proof-of-concept in the treatment of psoriasis. Int J Pharm. 2016; 500: 268-74.
15. Desai PR, Marepally S, Patel AR, Voshavar C, Chaudhuri A, Singh M. Topical delivery of anti-TNFα siRNA and capsaicin via novel lipid-polymer hybrid nanoparticles efficiently inhibits skin inflammation in vivo. J Controlled Release. 2013; 170: 51-63.
16. Petrilli R, Eloy JO, Praca FS, Del Ciampo JO, Fantini MA, Fonseca MJ, et al. Liquid Crystalline Nanodispersions Functionalized with Cell-Penetrating Peptides for Topical Delivery of Short-Interfering RNAs: A Proposal for Silencing a Pro-Inflammatory Cytokine in Cutaneous Diseases. Journal of biomedical nanotechnology. 2016; 12: 1063-75.
17. P. Shah P, R. Desai P, Channer D, Singh M. Enhanced skin permeation using polyarginine modified nanostructured lipid carriers. J Controlled Release. 2012; 161: 735-45.
18. Prausnitz MR. Microneedles for transdermal drug delivery. Advanced Drug Delivery Reviews. 2004; 56: 581-7.
19. Kabanov AV, Vinogradov SV. Nanogels as Pharmaceutical Carriers: Finite Networks of Infinite Capabilities. Angew Chem Int Ed. 2009; 48: 5418-29.
20. Asadian-Birjand M, Sousa-Herves A, Steinhilber D, Cuggino JC, Calderon M. Functional Nanogels for Biomedical Applications. Current Medicinal Chemistry. 2012; 19: 5029-43.
21. Morales-Cruz M, Flores-Fernández GM, Morales-Cruz M, Orellano EA, Rodriguez-Martinez JA, Ruiz M, et al. Two-step nanoprecipitation for the production of protein-loaded PLGA nanospheres. Results in Pharma Sciences. 2012; 2: 79-85.
22. Bilati U, Allémann E, Doelker E. Nanoprecipitation versus emulsion-based techniques for the encapsulation of proteins into biodegradable nanoparticles and process-related stability issues. AAPS PharmSciTech. 2005; 6: E594-E604.
23. Steinhilber D, Witting M, Zhang X, Staegemann M, Paulus F, Friess W, et al. Surfactant free preparation of biodegradable dendritic polyglycerol nanogels by inverse nanoprecipitation for encapsulation and release of pharmaceutical biomacromolecules. J Controlled Release. 2013; 169: 289-95.
24. Mease PJ, Goffe BS, Metz J, VanderStoep A, Finck B, Burge DJ. Etanercept in the treatment of psoriatic arthritis and psoriasis: a randomised trial. Lancet (London, England). 2000; 356: 385-90.
25. Moreland LW, Schiff MH, Baumgartner SW, Tindall EA, Fleischmann RM, Bulpitt KJ, et al. Etanercept therapy in rheumatoid arthritis. A randomized, controlled trial. Ann Intern Med. 1999; 130: 478-86.
26. Hönzke S, Wallmeyer L, Ostrowski A, Radbruch M, Mundhenk L, Schäfer-Korting M, et al. Influence of Th2 Cytokines on the Cornified Envelope, Tight Junction Proteins, and β-Defensins in Filaggrin-Deficient Skin Equivalents. Journal of Investigative Dermatology. 2016; 136: 631-9.
27. Hönzke S, Gerecke C, Elpelt A, Zhang N, Unbehauen M, Kral V, et al. Tailored dendritic core-multishell nanocarriers for efficient dermal drug delivery: A systematic top-down approach from synthesis to preclinical testing. J Controlled Release. 2016; 242: 50-63.
28. Bernard F-X, Morel F, Camus M, Pedretti N, Barrault C, Garnier J, et al. Keratinocytes under Fire of Proinflammatory Cytokines: Bona Fide Innate Immune Cells Involved in the Physiopathology of Chronic Atopic Dermatitis and Psoriasis. Journal of Allergy. 2012; 2012: 10.
29. Gerecke C, Edlich A, Giulbudagian M, Schumacher F, Zhang N, Said A, et al. Biocompatibility and characterization of polyglycerol-based thermoresponsive nanogels designed as novel drug-delivery systems and their intracellular localization in keratinocytes. Nanotoxicology. 2017; 11: 267-77.
30. Dommerholt J, Schmidt S, Temming R, Hendriks LJA, Rutjes FPJT, van Hest JCM, et al. Readily Accessible Bicyclononynes for Bioorthogonal Labeling and Three-Dimensional Imaging of Living Cells. Angew Chem Int Ed. 2010; 49: 9422-5.
31. Fischer W, Calderón M, Schulz A, Andreou I, Weber M, Haag R. Dendritic Polyglycerols with Oligoamine Shells Show Low Toxicity and High siRNA Transfection Efficiency in Vitro. Bioconjugate Chem. 2010; 21: 1744-52.
32. Gervais M, Brocas A-L, Cendejas G, Deffieux A, Carlotti S. Synthesis of Linear High Molar Mass Glycidol-Based Polymers by Monomer-Activated Anionic Polymerization. Macromolecules. 2010; 43: 1778-84.
33. Cuggino JC, Alvarez I CI, Strumia MC, Welker P, Licha K, Steinhilber D, et al. Thermosensitive nanogels based on dendritic polyglycerol and N-isopropylacrylamide for biomedical applications. Soft Matter. 2011; 7: 11259-66.
34. Kuchler S, Henkes D, Eckl KM, Ackermann K, Plendl J, Korting HC, et al. Hallmarks of atopic skin mimicked in vitro by means of a skin disease model based on FLG knock-down. Alternatives to laboratory animals : ATLA. 2011; 39: 471-80.
35. Said A, Bock S, Muller G, Weindl G. Inflammatory conditions distinctively alter immunological functions of Langerhans-like cells and dendritic cells in vitro. Immunology. 2015; 144: 218-30.
36. Schubert S, Delaney JJT, Schubert US. Nanoprecipitation and nanoformulation of polymers: from history to powerful possibilities beyond poly(lactic acid). Soft Matter. 2011; 7: 1581-8.
37. Hornig S, Heinze T, Becer CR, Schubert US. Synthetic polymeric nanoparticles by nanoprecipitation. J Mater Chem. 2009; 19: 3838-40.
38. Giulbudagian M, Asadian-Birjand M, Steinhilber D, Achazi K, Molina M, Calderon M. Fabrication of thermoresponsive nanogels by thermo-nanoprecipitation and in situ encapsulation of bioactives. Polymer Chemistry. 2014; 5: 6909-13.
39. Bilati U, Allémann E, Doelker E. Development of a nanoprecipitation method intended for the entrapment of hydrophilic drugs into nanoparticles. European Journal of Pharmaceutical Sciences. 2005; 24: 67-75.
40. Stainmesse S, Orecchioni A-M, Nakache E, Puisieux F, Fessi H. Formation and stabilization of a biodegradable polymeric colloidal suspension of nanoparticles. Colloid Polym Sci. 1995; 273: 505-11.
41. Kim NA, Lim DG, Lim JY, Kim KH, Jeong SH. Comprehensive evaluation of etanercept stability in various concentrations with biophysical assessment. Int J Pharm. 2014; 460: 108-18.
42. Maarschalkerweerd Av, Wolbink G-J, Stapel SO, Jiskoot W, Hawe A. Comparison of analytical methods to detect instability of etanercept during thermal stress testing. European Journal of Pharmaceutics and Biopharmaceutics. 2011; 78: 213-21.
43. Jung Y-S, Park W, Na K. Temperature-modulated noncovalent interaction controllable complex for the long-term delivery of etanercept to treat rheumatoid arthritis. J Controlled Release. 2013; 171: 143-51.
44. Seok J, Warren HS, Cuenca AG, Mindrinos MN, Baker HV, Xu W, et al. Genomic responses in mouse models poorly mimic human inflammatory diseases. Proceedings of the National Academy of Sciences. 2013; 110: 3507-12.
45. Gerber Peter A, Buhren Bettina A, Schrumpf H, Homey B, Zlotnik A, Hevezi P. The top skin-associated genes: a comparative analysis of human and mouse skin transcriptomes. Biol Chem; 2014. p. 577.
46. Perrin S. Preclinical research: Make mouse studies work. Nature. 2014; 507: 423-5.
47. Baliwag J, Barnes DH, Johnston A. Cytokines in psoriasis. Cytokine. 2015; 73: 342-50.
48. Ahrens K, Schunck M, Podda GF, Meingassner J, Stuetz A, Schroder JM, et al. Mechanical and metabolic injury to the skin barrier leads to increased expression of murine beta-defensin-1, -3, and -14. The Journal of investigative dermatology. 2011; 131: 443-52.
49. Wallmeyer L, Dietert K, Sochorová M, Gruber AD, Kleuser B, Vávrová K, et al. TSLP is a direct trigger for T cell migration in filaggrin-deficient skin equivalents. Scientific Reports. 2017; 7: 774.
50. Egawa G, Kabashima K. Multifactorial skin barrier deficiency and atopic dermatitis: Essential topics to prevent the atopic march. The Journal of allergy and clinical immunology. 2016; 138: 350-8.e1.
51. Gould AR, Sharp PJ, Smith DR, Stegink AJ, Chase CJ, Kovacs JC, et al. Increased permeability of psoriatic skin to the protein, plasminogen activator inhibitor 2. Arch Dermatol Res. 2003; 295: 249-54.
52. Bashir SJ, Chew A-L, Anigbogu A, Dreher F, Maibach HI. Physical and physiological effects of stratum corneum tape stripping. Skin Research and Technology. 2001; 7: 40-8.
53. Loryn E. Fechner MK, Maria Molina, Stefanie Wedepohl, Marcelo Calderón. Semi-interpenetrated polymeric near-infrared absorbing nanogels for efficient photothermal therapy of cancer. 11th Int Symp Polymer Therapeutic. Valencia, Spain; 2016.
54. Giulbudagian M, Rancan F, Klossek A, Yamamoto K, Jurisch J, Neto VC, et al. Correlation between the chemical composition of thermoresponsive nanogels and their interaction with the skin barrier. J Controlled Release. 2016; 243: 323-32.
55. Warner RR, Stone KJ, Boissy YL. Hydration disrupts human stratum corneum ultrastructure. The Journal of investigative dermatology. 2003; 120: 275-84.
56. Choi WI, Lee JH, Kim JY, Kim JC, Kim YH, Tae G. Efficient skin permeation of soluble proteins via flexible and functional nano-carrier. Journal of controlled release : official journal of the Controlled Release Society. 2012; 157: 272-8.
57. Zielinska K, Sun H, Campbell RA, Zarbakhsh A, Resmini M. Smart nanogels at the air/water interface: structural studies by neutron reflectivity. Nanoscale. 2016; 8: 4951-60.
58. Danso MO, van Drongelen V, Mulder A, van Esch J, Scott H, van Smeden J, et al. TNF-alpha and Th2 cytokines induce atopic dermatitis-like features on epidermal differentiation proteins and stratum corneum lipids in human skin equivalents. The Journal of investigative dermatology. 2014; 134: 1941-50.
59. Heath WR, Carbone FR. The skin-resident and migratory immune system in steady state and memory: innate lymphocytes, dendritic cells and T cells. Nature immunology. 2013; 14: 978-85.
60. Middleton MH, Norris DA. Cytokine-induced ICAM-1 expression in human keratinocytes is highly variable in keratinocyte strains from different donors. The Journal of investigative dermatology. 1995; 104: 489-96.
61. Xu W, Jia S, Xie P, Zhong A, Galiano RD, Mustoe TA, et al. The Expression of Proinflammatory Genes in Epidermal Keratinocytes Is Regulated by Hydration Status. Journal of Investigative Dermatology. 2014; 134: 1044-55.
62. Rancan F, Giulbudagian M, Jurisch J, Blume-Peytavi U, Calderon M, Vogt A. Drug delivery across intact and disrupted skin barrier: Identification of cell populations interacting with penetrated thermoresponsive nanogels. European journal of pharmaceutics and biopharmaceutics : official journal of

Arbeitsgemeinschaft fur Pharmazeutische Verfahrenstechnik eV. 2017; 116: 4-11.
63. Edlich A, Gerecke C, Giulbudagian M, Neumann F, Hedtrich S, Schafer-Korting M, et al. Specific uptake mechanisms of well-tolerated thermoresponsive polyglycerol-based nanogels in antigen-presenting cells of the skin. European journal of pharmaceutics and biopharmaceutics : official journal of Arbeitsgemeinschaft fur Pharmazeutische Verfahrenstechnik eV. 2017; 116: 155-63.
64. Gerecke C, Edlich A, Giulbudagian M, Schumacher F, Zhang N, Said A, et al. Biocompatibility and characterization of polyglycerol-based thermoresponsive nanogels designed as novel drug-delivery systems and their intracellular localization in keratinocytes. Nanotoxicology. 2017; 11: 267-77.
65. Li N, Peng LH, Chen X, Nakagawa S, Gao JQ. Transcutaneous vaccines: novel advances in technology and delivery for overcoming the barriers. Vaccine. 2011; 29: 6179-90.
66. Rancan F, Amselgruber S, Hadam S, Munier S, Pavot V, Verrier B, et al. Particle-based transcutaneous administration of HIV-1 p24 protein to human skin explants and targeting of epidermal antigen presenting cells. J Control Release. 2014; 176: 115-22.
67. Abdel-Mottaleb MM, Try C, Pellequer Y, Lamprecht A. Nanomedicine strategies for targeting skin inflammation. Nanomedicine (Lond). 2014; 9: 1727-43.